Anal. Bioanal. Electrochem., Vol. 7, No. 4, 2015, 509-522

Analytical & Bioanalytical Electrochemistry

2015 by CEE
www.abechem.com

Full Paper

Experimental and Quantum Chemical Evaluation of Dihydropyridine Derivative as Environmental Benign Corrosion Inhibitor for Mild Steel in 15% HCl

Kashif R. Ansari and Mumtaz A. Quraishi *

Department of Chemistry, Indian Institute of Technology (Banaras Hindu University), Varanasi -221005, India

* Corresponding Author, Tel.: +91-9307025126; Fax: +91- 542- 2368428

E-Mails: maquraishi@rediffmail.com, maquraishi.apc@itbhu.ac.in

Received: 1 July 2015 / Received in revised form: 23 July 2015 / Accepted: 14 August 2015 / Published online: 31 August 2015

Abstract- The behavior of 1,1'-{2, 6-dimethyl-4-[-2-phenylethenyl]-1,4-dihydropyridine-3,5-diyl}diethanone (DHP) have been investigated as mild steel (MS) corrosion inhibitor in 15% HCl solution by gravimetric measurements, electrochemical impedance spectroscopy (EIS), potentiodynamic polarization (Tafel), scanning electron microscopy (SEM) analysis. Quantum chemical calculation was applied to correlate electronic structure parameters with the inhibition performances. Adsorption of DHP obeys the Langmuir's isotherm. Potentiodynamic polarization measurements showed that DHP acted as mixed type inhibitor but cathodically dominant

Keywords- EIS, SEM, Quantum chemical calculation, Mild steel (MS)

1. INTRODUCTION

In the chemical industries, huge amount of HCl is being used for removal of undesired scales and rust which are present on the MS surface. However, during this process detoriation of MS occurs. In order to reduce the MS destruction inhibitors are added. The addition of

corrosion inhibitors effectively protect the MS against acid attack. Many studies in this regard using organic inhibitors have been reported [1,2].

Now a day's, much focus has been directed towards the development of non-toxic inhibitors for the environmental safety purpose. Keeping this in mind, we have carried out the synthesis of 1, 1'-{2, 6-dimethyl-4-[-2-phenylethenyl]-1,4-dihydropyridine-3,5-diyl}diethanone. This compound is acting as a nucleus for medicines, which is used in congestive heart failure and shows cytotoxic activity against human-oral squamous carcinoma. In addition to these biological activities, it is acting as a good corrosion inhibitor in stronger acidic and high temperature conditions. The literature survey reveals that several pyridine derivatives were used as corrosion inhibitors [3-9].

Most of the corrosion inhibitors used previously is effective at lower acid concentration [10-12]. However, most commonly 15% HCl is used for scale and rust removable from mild steel. Therefore, keeping the above said statement and continuation of our interest in the development of corrosion inhibitor in hot and concentrated acid [13-16], we are reporting here the inhibitory performance of dihydropyridine derivative namely 1, 1'-{2, 6-dimethyl-4-[-2-phenylethenyl]-1,4-dihydropyridine-3,5-diyl}diethanone (DHP) on the corrosion of MS in 15% HCl. This compound is first time used as a corrosion inhibitor for MS in 15% HCl. The inhibitive activity of inhibitor was examined successively via gravimetric measurement, electrochemical impedance spectroscopy (EIS), Tafel polarization, Langmuir isotherm, scanning electron microscopy (SEM) and Quantum chemical calculation.

2. MATERIALS AND METHODS

2.1. General

The inhibitor was synthesized according to the procedure given elsewhere [17] and is given in Fig. 1. The inhibitor was recrystallized from ethanol.

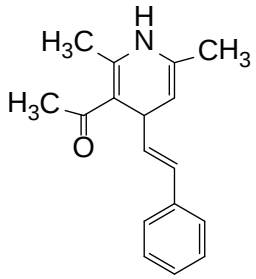

Fig. 1. Molecular structure of DHP

The MS strips having composition (wt.%) of 0.17 wt.% C, 0.37 wt.% Mn, 0.20 wt.% Si, 0.03 wt.% S, 0.01 wt.% P and remaining Fe. MS with an area of 30.1 cm^2 and 1 cm^2 were used for gravimetric and electrochemical studies respectively. The surface of the MS

specimens were abraded with emery papers (grade 600 to 1200), which was then washed in deionized water and then dried at room temperature. The test solution (15% HCl) volume/volume (v/v) was prepared by diluting 37% analytical grade HCl with double distilled water.

2.2. Gravimetric measurement

Gravimetric measurement was done according to ASTM method [18]. The MS strips were immersed in 100 mL (15%) HCl in absence and presence of DHP. After immersion for 6 h at 308 and 323 K and also at 378 K for 0.5 h MS strips were taken out, washed, dried, and then weighed accurately. The value of corrosion rate C_R (mg cm^{-2} h^{-1}), surface coverage (θ) and inhibition efficiency (η %) were calculated from the following equations [19].

$$C_R = \frac{W}{At} \quad (1)$$

$$\theta = \frac{C_R - C_{R(i)}}{C_R} \quad (2)$$

$$\eta\% = \frac{C_R - C_{R(i)}}{C_R} \times 100 \quad (3)$$

Where W is the weight loss, A is the total area, t is immersion time, C_R and $C_{R(i)}$ are corrosion rates (mg cm^{-2} h^{-1}) of MS strip in the absence and presence of DHP respectively.

2.3. Electrochemical measurements

The electrochemical measurements were carried out using a conventional three-electrode cell assembly at 308 K. In which MS strips, platinum and saturated calomel (SCE) were used as the working, counter and reference electrodes respectively. Prior to the measurement working electrode was immersed in the test solution (15%) HCl in absence and presence of inhibitor for 30 min until a steady potential was reached.

In order to find the potentiodynamic polarization curves the electrode potential was changed from -250 to +250 mV versus SCE at OCP at a sweep rate of 1 mVs^{-1}. Impedance measurements were carried out using AC signals of amplitude 10 mV peak to peak at the open circuit potential in the frequency range 100 kHz to 0.01 Hz. All impedance data were fitted to appropriate circuits using the computer program Echem Analyst 5.0. All electrochemical measurements were carried out using a Gamry Potentiostat /Galvanostat (Model G-300) connected with a personal computer with EIS software Gamry Instruments Inc., USA. The electrochemical experiments were analyzed by electrochemical software Echem Analyst 5.0 software package. These electrochemical measurements i.e. potentiodynamic polarization and Impedance measurements were carried out at 308 K.

2.4. Surface analysis

In order to find out the surface morphology of the MS specimens in absence and presence of DHP, MS specimens were exposed to 15% HCl solution in the absence and presence of optimum concentrations (400 and 2000 mg/L) of inhibitor for 6 h at 308 K and 0.5 h at 378 K immersion respectively. SEM was investigated by using Ziess Evo 50 XVP instrument at an accelerating voltage of 5 kV and 5 K X magnification.

2.5. Quantum chemical calculations

In the present work, Quantum chemical calculations were carried out by using density function theory (DFT) method, with the Gaussian-03 program [20]. The exchange-correlation was treated using hybrid, B3LYP functional. Optimization of molecule was done by using the 6-31G (d, p) basis sets. Various quantum chemical parameters like E_{HOMO}, E_{LUMO}, $\Delta E_{LUMO-HOMO}$, the dipole moment (μ) and Mulliken charges on heteroatoms of both neutral and protonated molecule were discussed.

3. RESULTS AND DISCUSSION

3.1. Gravimetric measurements

The values of inhibition efficiency (η %) with different concentration, temperature and time is given in Fig. 2.

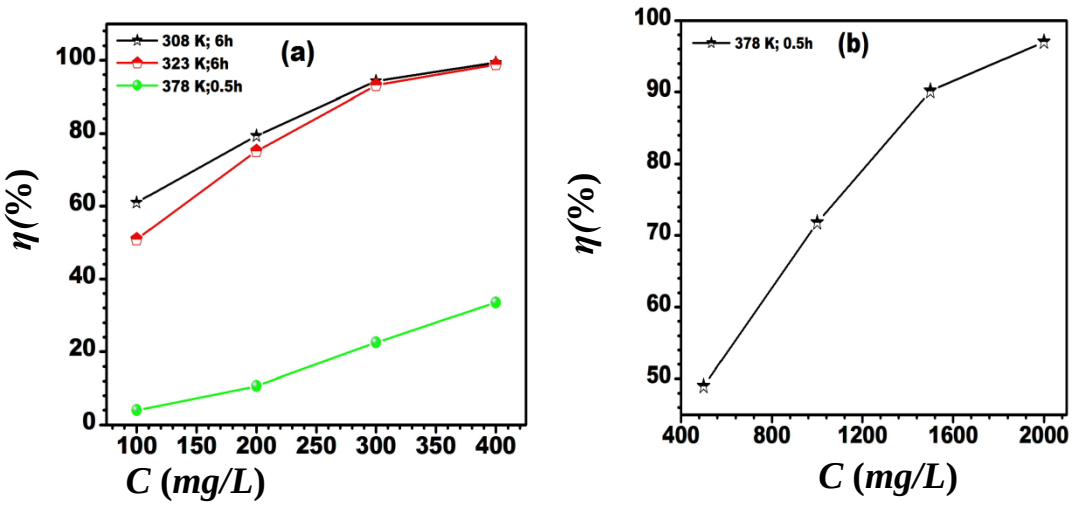

Fig. 2. Variation of inhibition efficiency (a) at lower concentration (b) at higher concentration

Fig. 2 (a-b) reveals that the inhibition efficiency (η %) increases with the increase in DHP concentration. Also as the temperature increases there is decrease in inhibition efficiency

occurs. The highest decrease in inhibition efficiency (η %) occurs at 378 K for 0.5 h. In order to enhance the corrosion inhibition ability of DHP at higher temperature (378 K), the concentration of inhibitor was increased up to 2000 mg/L and the efficiency goes to 97.03% [Fig. 2 (b)].

3.2. Adsorption considerations

Adsorption isotherm provides useful insights into the mechanism of corrosion inhibition. To find out the adsorption of DHP on MS surface different adsorption isotherms were tested. But out of these only Langmuir adsorption isotherm was found to be best fit (Fig. 3) and it can be given by the following equation [21]:

$$C/\theta = 1/K_{ads} + C \tag{4}$$

where θ is the surface coverage, C is the inhibitor concentration, K_{ads} is the equilibrium constant of adsorption process.

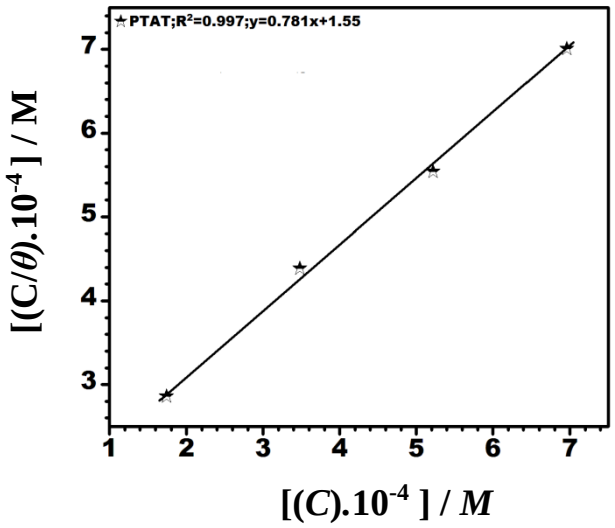

Fig. 3. Langmuir's isotherm plots for adsorption of DHP on MS surface in 15% HCl at 308 K

By using the intercepts of the straight lines K_{ads} can be calculated and its correlation with the standard free energy of adsorption ($\Delta G°_{ads}$) can be given by the following equation [22]

$$\Delta G^{o}_{ads} = -RT \ln(55.5K_{ads}) \tag{5}$$

Where *R* is the gas constant and *T* is the absolute temperature. The value of 55.5 is the concentration of water in solution in mol L^{-1}. The correlation coefficient value (R^2=0.997) is approaching to 1, which supports the best fitting of Langmuir adsorption isotherm (Fig. 3).

The values of K_{ads} and $\Delta G°_{ads}$ are 6.45×10^3 M^{-1} and -32.75 kJ mol^{-1} respectively. Previously many authors said that when the values of $\Delta G°_{ads}$ goes up to -20 kJ mol^{-1} are consistent with the electrostatic interaction between the charged molecules and the charged metal (physical adsorption) while those more negative than -40 kJ mol^{-1} involve the sharing or transfer of electrons from the inhibitor molecules to the metal surface to form a co-ordinate type of bond (chemisorption) [23]. In present study, the value of $\Delta G°_{ads}$ is in between -20 kJ mol^{-1} and -40 kJ mol^{-1}, which reveals that DHP adsorbed on the MS surface by a co-operation phenomenon between chemisorption and physisorption.

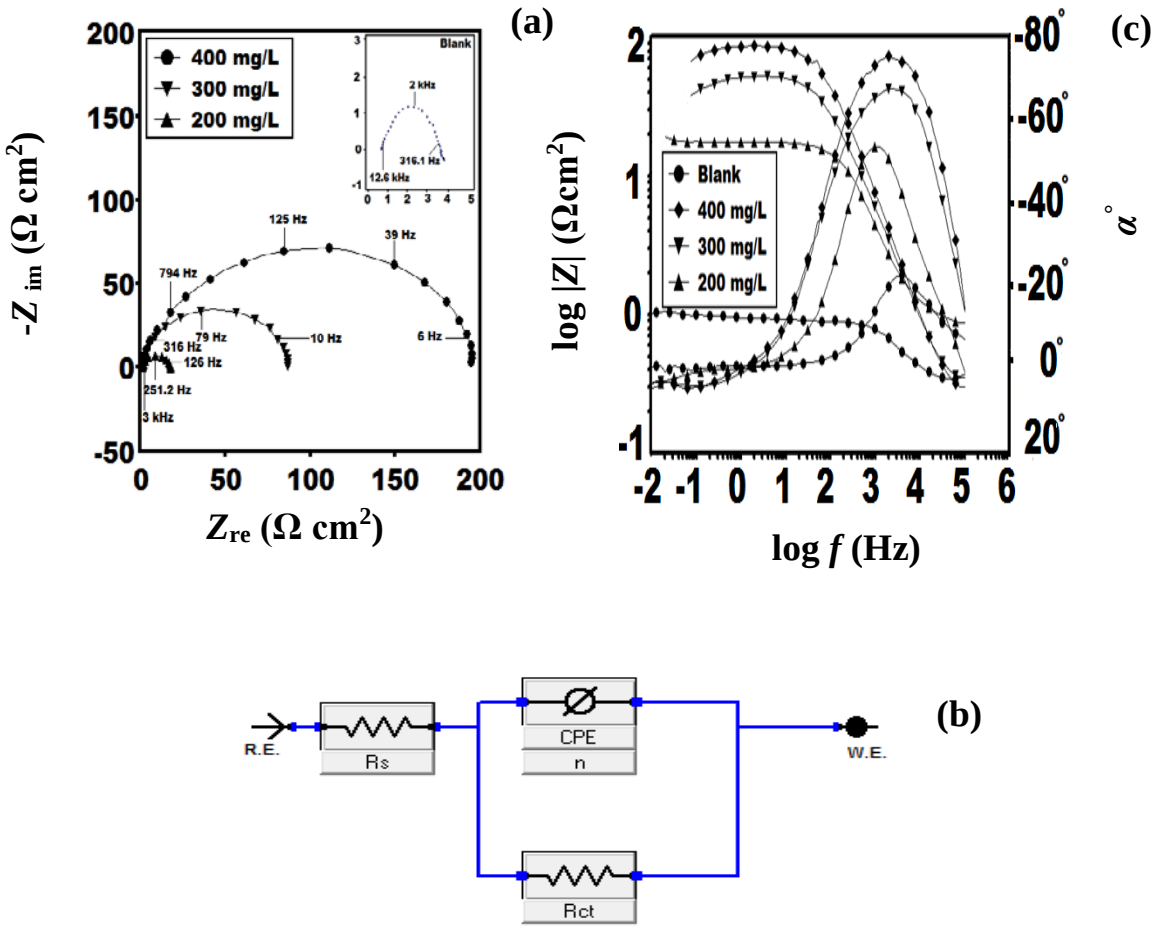

Fig. 4. a) Nyquist plots for MS in 15% HCl in absence and presence of different concentration of DHP at 308 K; **b)** Equivalent circuit model used to fit the EIS data; **c)** Bode (log f vs. log |Z|) and phase angle (log f vs. α◦) plots of impendence spectra for MS in 15% HCl in absence and presence of different concentration of DHP at 308 K

3.3. Electrochemical measurements

3.3.1. Electrochemical impedance spectroscopy

The corrosion behavior of MS in 15% HCl solution in the absence and presence of DHP at 308 K was investigated by the electrochemical impedance spectroscopy. Nyquist plots of MS were given in Fig. 4 (a). Inception of Fig. 4(a) suggests that at every concentration a single depressed semicircle is observed, which reveals that the charge transfer process is occurring at electrode/solution interface [24]. These impedance diagrams are not perfect semicircle, which indicates towards the frequency dispersion due to the roughness and in homogeneousness of the MS surface [25,26]. Also the impedance response in absence and presence of DHP are quite different i.e. bigger in presence of DHP than in its absence and also increases as the concentration of DHP increases.

In order to extract the results from Nyquist plots, an equivalent circuit was used Fig. 4 (b) which consists of solution resistance (R_s), a charge transfer resistance (R_{ct}) and a constant phase element (CPE). Constant phase element (CPE) is used in place of capacitor in electrochemical process in order to deal with the non-ideal capacitance response. [25]. R_s, R_{ct}, CPE and CPE exponent (n) values in 15% HCl in absence and presence of different concentration of DHP at 308 K were listed in Table 1.

Table 1. Electrochemical impedance parameters in 15% HCl solution in the absence and presence of different concentration of DHP at 308 K

C (mgL^{-1})	R_s (Ω)	R_{ct} (Ω cm^2)	n ($\mu F/cm^2$)	C_{dl} (%)	η
Blank	0.315	3.66	0.761	127.96	--
200	0.893	16.13	0.848	47.21	77.28
300	0.242	85.19	0.896	27.98	95.69
400	0.235	193.06	0.840	7.94	98.10

The inhibition efficiencies from R_{ct} were calculated by using the following equation [27,28]:

$$\eta\% = \left(1 - \frac{R_{ct}}{R_{ct(t)}}\right) \quad (6)$$

Where R_{ct} and $R_{ct(i)}$ are the charge transfer resistance in absence and presence of different concentration of inhibitor. As the concentration of DHP was increased, the R_{ct} values increased and C_{dl} decreased (Table 1) [29].

This decrease in the C_{dl} values occurs due to the decrease in local dielectric constant and/or an increase in the thickness of the electrical double layer, which reveals that the action of DHP molecules at the metal/solution interface occurs by adsorption [27].

In Bode plots log |*Z*| and phase angle ($\alpha°$) are plotted against log *f* as shown in Fig. 4 (c).

A linear relationship between log |*Z*| *vs*. log *f* with a slope value of -1 has to be obtained at intermediate frequencies for pure capacitive behavior. At intermediate frequencies, log |*Z*| *vs*. log *f* with slope and maximum phase angle values ($\alpha°$) are listed in Table 2.

In case of an ideal capacitive behavior the slope and phase angle ($\alpha°$) values are -1 of -90° respectively. The observation of Table 2 reveals that slopes of Bode impedance magnitude (-*S*) and maximum phase angle values shifting towards -1 and -90° as the concentration increases. This deviations in slopes of Bode impedance magnitude (-*S*) and the phase angles *($\alpha°$)* occurs because of the non- ideal capacitive behavior at intermediate frequencies. But as the concentration of DHP increases -*S* and $\alpha°$ values were approaching towards the ideal capacitive values.

Table 2. The slopes of the Bode impedance magnitude plots at intermediate frequencies (*S*) and the maximum phase angles ($\alpha°$) in 15% HCl solution in the absence and presence of different concentration of DHP at 308 K

C_{inh} (mg L^{-1})	- *S*	- $\alpha°$
Blank	0.317	22.60
2	0.705	53.64
300	0.769	67.71
400	0.862	75.58

3.3.2. Potentiodynamic polarization

Tafel Polarization curves of MS in 15% HCl in the absence and presence of different concentrations of DHP at 308 K is shown in Fig. 5.

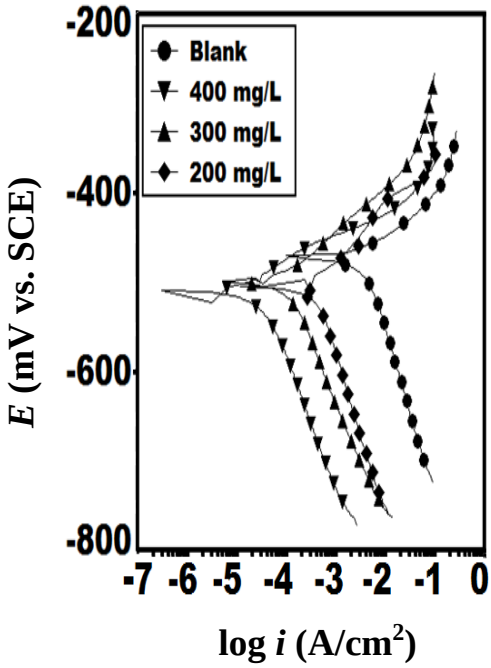

Fig. 5. Tafel curves for MS in 15% HCl in absence and presence of different concentration of DHP at 308 K

The inspection of Fig. 5 reveals that the corrosion potentials (E_{corr}) shifts towards more negative direction in the presence of DHP and cathodic curves are shifted to lower current density region compared to that of the blank solution, which results in I_{corr} values to decrease. This phenomenon clearly indicates that DHP acts as a cathodic inhibitor for MS in HCl solution. But also the anodic curves shift towards the lower current densities. So, a conclusion can be drawn that the DHP can retard both the anodic MS dissolution and cathodic hydrogen evolution reactions simultaneously. Thus overall DHP acting as a mixed type, but pre-dominantly suppressing the cathodic reaction [29]. Inhibition efficiency (η %) can be calculated using Eq. (7) [30]:

$$\eta\% = \left(1 - \frac{I_{corr(i)}}{I_{corr}}\right) \times 100 \quad (7)$$

Where I_{corr} and $I_{corr(i)}$ are the uninhibited and inhibited corrosion current densities, respectively.

Tafel parameters such as Corrosion potential (E_{corr}), cathodic Tafel slopes (β_c), anodic Tafel slopes (β_a) and corrosion current density (I_{corr}) can be obtained by exapulating the Tafel curves and are given in Table 3.

Table 3. Electrochemical polarization parameters in 15% HCl solution in the absence and presence of different concentrations of DHP at 308 K

Inhibitor	E_{corr} (mV/SCE)	I_{corr} (μA/cm^2)	β_a (mV/dec)	$-\beta_c$ (mV/dec)	η (%)
Blank					--
	-471	3630	55	185	
200	-504	707	82	161	80.52
300	-503	124	60	157	96.58
400	-509	5	61	150	99.86

It is apparent from Table 3 that, there is a significant decrease in the I_{corr} values after the addition of DHP and increases as DHP concentration increases, which reveals the formation of a protective film of DHP on the MS surface.

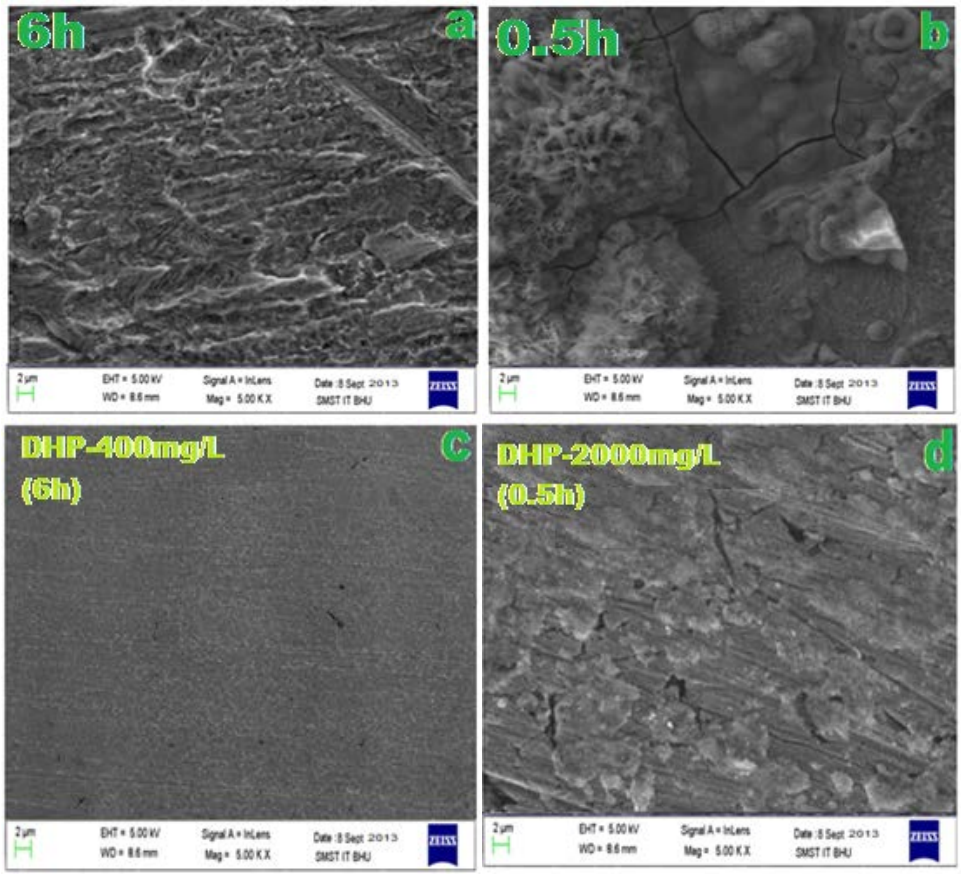

Fig. 6. a-d: SEM micrographs of MS surfaces (a) uninhibited 15% HCl (6h) at 308 K (b) uninhibited 15% HCl (0.5h) at 378 K (c) DHP (400 mg/L) for 6h at 308 K (d) DHP (2000 mg/L) for 0.5h at 378 K

3.4. Surface characterization: SEM

SEM micrographs of MS after immersing in 15% HCl in the absence and presence of optimum concentration (400 and 2000 mg/L) of DHP at 308 K and 378 K for 6h and 0.5h respectively were shown in Fig. 6 (a-d).

3.5. Quantum chemical calculations

3.5.1. Neutral inhibitor

The electronic parameters such as E_{HOMO}, E_{LUMO}, ΔE, dipole moment (μ) and Mulliken charges on hetero-atoms have calculated and are listed in Table 4.

Table 4. Calculated quantum chemical parameters

Inhibitors	μ (Debye)	E_{HOMO} (eV)	E_{LUMO} (eV)	ΔE (eV)	N_6	O_{19}
DHP	5.073	-3.538	-1.080	2.458	-0.803	-0.377
DHP^+	9.023	-3.447	-1.888	1.559	-0.739	-0.353

The optimized structure of neutral and protonated DHP, E_{HOMO} and E_{LUMO} are shown in Fig. 7 (a-c).

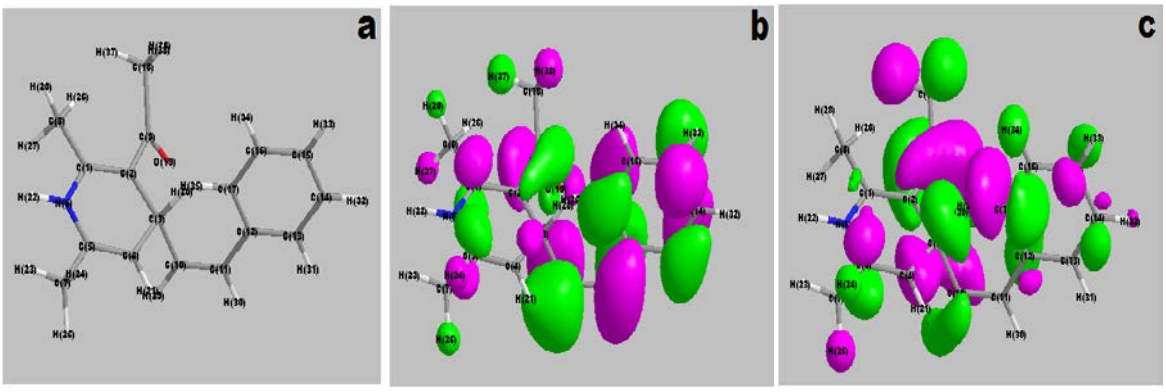

Fig. 7. (a) Optimized structure (b) HOMO (c) LUMO

In general E_{HOMO} and E_{LUMO} are the electronic parameter which indicates the tendency of the molecule to donate and accept the electrons i.e. higher the E_{HOMO} value greater is the ability of the molecule to donate the electrons and lower the E_{LUMO} value greater is the ability of the molecule to accept the electrons [31,32]. The observation of Table 4 reveals that E_{HOMO} value is large and E_{LUMO} value is small.

The other important electronic parameter is energy gap (ΔE), which indicates the reactivity of molecule towards metal surface. The smaller the value of ΔE greater will be the reactivity of the molecule, which favors the adsorption of the molecule [23]. As the ΔE gap is small, there will be easy transfer of the electrons from the E_{HOMO} to E_{LUMO} and thus stronger will be the adsorption of the molecule over the metal surface. Table 4 shows that the value of ΔE is small enough for the easy transfer of the electrons from the E_{HOMO} to E_{LUMO} and provide stronger adsorption of DHP molecule on MS surface. The larger value of dipole moment (μ) also favors the adsorption of DHP molecule. Table 4 shows the calculated values of the Mulliken charges on hetero-atoms i.e. N and O, the negative charge on hetero-atoms indicates that these are the prominent sites for the adsorption on the MS surface either by physiosorption or chemisorption.

3.5.2. Protonated inhibitor

E_{HOMO} and E_{LUMO} are shown in Fig. 8 (a-c).

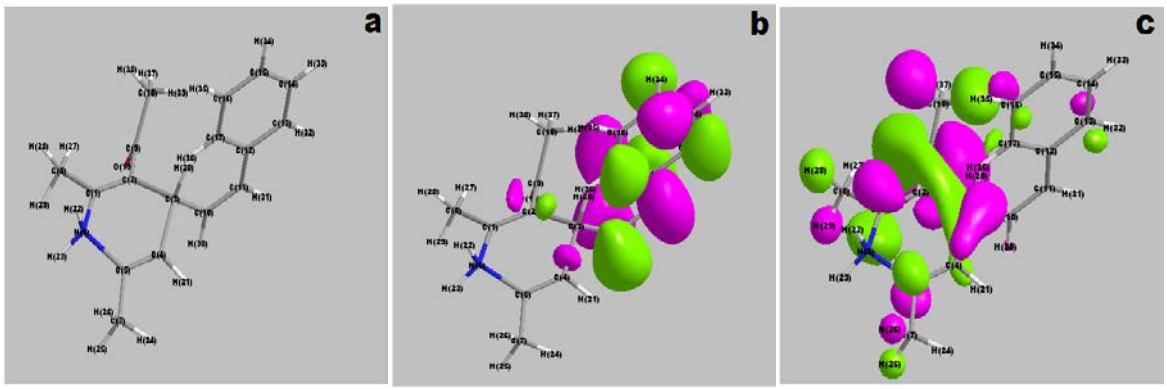

Fig. 8. (a) Optimized structure (b) HOMO (c) LUMO

In aqueous medium the inhibitor molecule undergoes protonation and these protonated species also adsorb on the MS surface. So, it will be important to compare the electronic properties of the protonated species with that of the neutral one in order to check which one will get adsorb on the metal surface dominantly. In the present case Mulliken charge on N atom is more negative as compared to O. So, this N atom gets protonated and the quantum chemical parameters of the preferred protonated species are given in Table 4.

After comparing the quantum chemical parameter of neutral and protonated DPH, we could say that the E_{HOMO} value is higher in protonated one as compared to the neutral one. This revealed that the protonated one has greater tendency to donate the electrons to MS and thus it could bind strongly on it. Also ΔE value in protonated one is lower than the neutral one, which further revealed that protonated one is more reactive than neutral one. Thus, overall it could said that protonated species are more likely to get adsorb over MS than

neutral one. The above discussion also supports the experimentally observed adsorption i.e. both physical and chemical.

3.6. Mechanism of inhibition

The mechanism of inhibition on the basis of quantum chemical calculation can be explained. In HCl medium DHP may either exists as a protonated (cation) or neutral species and these two species are in equilibrium with each other. Also MS is positively charged in HCl with respect to the potential of zero charge (PZC). So, three processes may involve during adsorption: (i) Cationic form of DHP undergoes electrostatic interaction with the Cl^{-1} ions which are initially adsorbed, (ii) Unshared electron pairs presenting on hetero-atoms interact with the vacant d-orbital of iron atoms. (iii) Retero-donation between the π-electrons of aromatic ring presenting in the DHP and vacant d-orbital of iron atoms presenting on the MS.

4. CONCLUSION

1. DHP is an effective corrosion inhibitor for MS in 15% HCl and the inhibition efficiency increases with increasing inhibitor concentration.
2. Data obtained from gravimetric and electrochemical measurements are strongly comparable.
3. SEM micrograph shows the formation of protective film of DHP over the MS surface.
4. DHP is acting as a mixed type inhibitor predominantly cathodic.
5. DHP obeys Langmuir's adsorption isotherm.
6. At higher temperature higher (378 K) concentration of DHP is required for better inhibition.

Acknowledgement

K. R. Ansari thanks to Ministry of Human Resource and Development (MHRD), New Delhi, India for the financial assistance.

REFERENCES

[1] A. O. Yüce, B. D. Mert, G. Kardas, and B. Yazıcı, Corros. Sci. 83 (2014) 310.
[2] K. R. Ansari, M. A. Quraishi, and A. Singh, Corros. Sci. 79 (2014) 5.
[3] S. A. Abd El-Maksoud, and A. S. Fouda, Mater. Chem. Phys. 93 (2005) 84.
[4] M. Doddahosuru. Gurudatt, and K. N. Mohana, Ind. Eng. Chem. Res. 53 (2014) 2092.
[5] A. Ghazoui, R. Saddik, N. Benchat, M. Guenbour, B. Hammouti, S. S. Al-Deyab, and A. Zarrouk, Int. J. Electrochem. Sci. 7 (2012) 7080.

[6] O. Krim, A. Elidrissi, B. Hammouti, A. Ouslim, and M. Benkaddour, Chem. Eng. Comm. 196 (2009) 1536.
[7] X. Li, X. Xie, S. Deng, and G. Duc, Corros. Sci. 87 (2014) 27.
[8] R. Yıldız, A. Dönerb, T. Doğanc, and İ. Dehria, Corros. Sci. 82 (2014) 125.
[9] B. D. Mert, A. O. Yüce, G. Kardaş, and B. Yazıcı, Corros. Sci. 85 (2014) 287.
[10] D. G. Ladha, P. M. Wadhwani, M. Y. Lone, P. C. Jha, and N. K. Shah, Anal. Bioanal. Electrochem. 7 (2015) 59.
[11] A. Fattah-alhosseini, A. Moradi, E. Moradi, and N. Attarzadeh, Anal. Bioanal. Electrochem. 6 (2014) 284.
[12] C. B. Verma, M. J. Reddy, and M. A. Quraishi, Anal. Bioanal. Electrochem. 6 (2014) 515.
[13] M. Ajmal, J. Rawat, and M. A. Quraishi. Anti-Coros. Mater. 45 (1998) 419.
[14] M. Ajmal, J. Rawat, and M. A. Quraishi, Bull. Electrochem. 15 (1999) 8.
[15] M. Ajmal, J. Rawat, and M. A. Quraishi, Bull. Electrochem. 14 (1998) 199.
[16] M. A. Quraishi, J. Rawat, and M. Ajmal, Corrosion 54 (1998) 996.
[17] V. N. Mathi, and A. J. S. S.Chitrabala, Int. J. Pharm. Pharm. Sci. 4 (2012) 651.
[18] ASTM (1990), G 31-72, American Society for Testing and Materials, Philadelphia, PA.
[19] X. Li, S. Deng, H. Fu, and T. Li, Electrochim. Acta 54 (2009) 4089.
[20] Gaussian 03, Revision E.01, M.J. Frisch et.al (2007) Gaussian Inc., Wallingford CT.
[21] K. R. Ansari, M. A. Quraishi, and A. Singh, Corros. Sci. 95 (2015) 62.
[22] K. R. Ansari, Sudheer, A. Singh, and M. A. J. Dispersion Sci. Technol. 36 (2015) 908.
[23] K. R. Ansari, and M. A. Quraishi, J. Taiwan. Inst. Chem. Eng. (2015) DOI.org/10.1016/j.jtice.2015.03.013.
[24] F. Bentiss, M. Traisnel, H. Vezin, H. F. Hildebrand, and M. Lagren, Corros. Sci. 46 (2004) 278.
[25] Q. Qu, Z. Hao, L. Li, W. Bai, and Z. Ding, Corros. Sci. 51 (2009) 569.
[26] B.M. Mistry, and S. Jauhari, J. Dispersion Sci. Technol. 34 (2013) 1758.
[27] K. R. Ansari, and M. A. Quraishi, J. Ind. Eng. Chem. 20 (2014) 2819.
[28] K. R. Ansari, and M. A. Quraishi, Physica E 69 (2015) 322.
[29] K. R. Ansari, and M. A. Quraishi, J. of the Assoc. of Arab Univ. for Basic and Appl. Sci. (2014) DOI.org/10.1016/j.jaubas.2014.04.001.
[30] K. R. Ansari, M. A. Quraishi, and A. Singh, J. Ind. Eng. Chem. 25 (2015) 89.
[31] I. B. Obot, and Z. M. Gasem, Corros. Sci. 83 (2014) 359.
[32] S. Deng, X. Li, and X. Xie, Corros. Sci. 80 (2014) 276.